Final, accepted. OCP

8.4.99

Femtosecond photoionization of $(H_2O)_n$ and $(D_2O)_n$ clusters

P. P. Radi, P. Beaud, D. Franzke, H-M. Frey, T. Gerber, B. Mischler, A-P. Tzannis

General Energy Research, Paul Scherrer Institute, CH-5232 Villigen, Switzerland

Cluster ion distributions of water in a molecular beam are investigated by using femtosecond ionization at 780 nm and reflectron time-of-flight mass spectrometry. The electric field strength generated by the ultrashort laser pulses is sufficient to ionize efficiently most of the molecules that are present in the molecular beam. In this work ion signals of large water clusters containing up to 60 monomers are reported. Upon ionization rapid proton transfer is observed leading to the formation of protonated water cluster ions. Unprotonated clusters, $(H_2O)_n^+$ (n>2), are not observed in the mass spectra. The configurational energy imparted into the protonated clusters induces unimolecular dissociation on the μs time scale. These metastable reactions are characterized by modeling the ion trajectories in the mass spectrometer. The numerical procedure in conjunction with the integrated parent and daughter intensities results in unimolecular dissociation rates as a function of cluster size. Additional information about proton transfer reactions is obtained by the investigation of deuterium substitutions. Even though these substitutions correspond to large relative changes in the mass of the atom as well as the zero point energy, unprotonated $(D_2O)_n^+$ clusters are not produced with significant abundance in supersonic expansions of deuterated water. An additional result of this work is the observation of doubly charged ions above a critical cluster size ($n \approx 37$).

INTRODUCTION

Water cluster series have been observed by electron impact ionization [1,2], free jet expansion of ionized water [3] and high energy bombardment of ice crystals [4]. Typically, the mass spectra of water clusters are dominated by protonated cluster ions, $(H_2O)_nH^+$, which are produced by rapid proton transfer:

$$(H_2O)_n + h\nu \rightarrow [(H_2O)_n^+]^* + e^- \rightarrow (H_2O)_{n-1}H^+ + OH + e^- \qquad (1)$$

where $[(H_2O)_n^+]^*$ stands for the vertically ionized water cluster. *Ab initio* potential energy calculations for the water dimer [5] show that the dimer cation exhibits quite a different geometry from that of the neutral dimer. The potential minima of the ground and first excited state of the cation are far from the wide Franck-Condon region expected from the shallow potential minimum of the neutral dimer. Proton transfer relaxation from the vertically ionized point to the potential minimum may easily occur with no activation barrier. Furthermore, the calculations indicate that the dissociation energy into the energetically lowest fragment channel leading to $H_3O^+ + OH$ lies slightly below the energy of the region reached by the vertical ionization process.

For the trimer and larger clusters an additional relaxation channel opens since they have single, weakly bound water molecules on their surface. As mentioned above, the vertical ionization energy of a water dimer unit in the cluster is much larger than the adiabatic value, since the geometry of the neutral and the ionized dimer differ considerably. In view of the dimer situation, substantial geometry changes are also expected for larger cluster, $(H_2O)_n^+ \geq 3$. After ionization, water molecules within the cluster will rearrange rapidly and release a large amount of energy. The high mobility of the proton might promote this process. As a consequence, the configurational energy imparted into the protonated cluster ion leads to the loss of one or several water monomers by metastable dissociation. Intensity anomalies observed in the mass spectra for $(H_2O)_{21}H^+$ and $(H_2O)_{28}H^+$ have been attributed to the metastable unimolecular decay on the μs time scale [2]. More recently, unprotonated cluster ions ($2 \leq n \leq 10$) have been detected by applying near-threshold photoionization at 11.83 eV on supersonic cluster beams of water-argon mixtures ($P \geq 2$ atm) [6]. It has been found that the unprotonated cluster ions $(H_2O)_n^+$ are produced *via* the photoionization of binary clusters:

$$(Ar)_m(H_2O)_n + h\nu \rightarrow (H_2O)_n^+ + m(Ar) + e^- \quad (2)$$

The authors rationalize their findings by randomization of the excess energy within the binary cluster. The excess energy is finally converted to the removal of argon atoms, giving rise to stable $(H_2O)_n^+$ (Reaction 2) and various $(Ar)_k(H_2O)_n^+$ ions.

Herein, we report on the femtosecond ionization at 780 nm of $(H_2O)_n$ and $(D_2O)_n$ clusters in a supersonic molecular beam that is coupled to a reflectron time-of-flight mass spectrometer. In general, the use of femtosecond laser pulses give rise to ionization pathways distinct from nanosecond excitation processes. The ultrashort pulse width combined with the high intensity ($\approx 10^{15}$ W cm^{-2}) of the light source permits excitation to the ionization state on a time scale which competes with nuclear motion. The electric field generated by the laser pulse is $E_0=(2I/\varepsilon_0 c)^{1/2}$, where E_o is the electric field strength (V m^{-1}), I is the intensity of the laser beam (W m^{-2}), ε_0 is the permittivity of free space, and c is the speed of light. Thus, the laser intensity corresponds to an electric field strength of $\approx$ 8.7 V Å^{-1} which is sufficient to ionize most of the molecules [7]. In fact, we demonstrate in this work that femtosecond laser pulses are producing protonated $(H_2O)_nH^+$ and $(D_2O)_nD^+$ clusters series readily observable up to n $\approx$ 60.

As mentioned above, the excess energy imparted into the cluster ions upon the vertical ionization and proton transfer process leads to metastable dissociation. This unimolecular decay on the μs time scale yields intensity anomalies ("magic numbers") in the mass spectrum. The dynamics of the decay is characterized by taking into account numerical simulations of the ion trajectories in the mass spectrometer. The results are in agreement with the findings reported by using electron-impact ionization [2]. In addition to singly charged cluster ions, doubly charged ions are observed and will be discussed in this work.

EXPERIMENT

A Ti:Sapphire laser system making use of the chirped pulse amplification technique (CPA 1000, Clark MXR, Dexter MI) produces bandwidth limited output pulses that have a duration of 95 fs (assuming a Gaussian pulse shape) and a bandwidth of 9 nm. Typical pulse energies are 250 μJ at a wavelength centered around 780 nm. The femtosecond pulses are focused into the source

chamber to a diameter of < 20 μm to give an intensity on the order of 10^{15} W cm^{-2}. The pulses intersect the supersonic molecular beam containing the neutral water clusters seeded in He, Ne or Ar . The ions formed in the ionization process are accelerated in an electric field and directed through the first field-free region towards the reflector. Ions are then reflected and travel through the second field-free region and are detected by a microchannel plate detector. The resolution of the mass spectrometer, m/Δm, is not optimized for reasons mentioned below and is typically 750 at m/e=200, where m is the mass of the ion and e the charge. Absolute calibration of the mass scale is performed by using the small impurities present in the beam (N_2, O_2) that are ionized efficiently with the fs laser pulses. Thus, a resolution of one mass unit which is required in this experiment is well attained for the significant mass range. If an ion fragments within the first field-free region, the daughter ion kinetic energy is defined by $U_e=(M_d/M_p)U_0$, where U_0 is the birth potential, M_d and M_p are the daughter and parent ion masses, respectively. By using appropriate reflector potentials, daughter and parent ions are reflected at different positions in the reflectron. In this way, parent and daughter ions of the same mass experience different trajectories and yield time-of-flights that are separated substantially.

Analysis of the metastable dissociation processes observed in the experimental spectra of the water cluster distributions is achieved by comparing the results with simulations of the ion trajectories in the mass spectrometer (SIMION [8]). The geometry and potentials of the electrodes are used to determine the electrostatic fields present in the apparatus by solving the Laplace equation by finite difference methods. By computing the electrostatic forces acting on a size selected parent cluster ion, the trajectory along the flight path is obtained and provides the time-of-flight, t_P. In a second step, the unimolecular dissociation of a metastable parent ion in the first field-free region is modeled and yields the time-of-flight of the daughter ion, t_D. The computation is iterated over all cluster sizes n resulting in $t_P(n)$ and $t_D(n)$. It is found that these time-of-flights reproduce the experimental observations accurately without any adjustment parameters. The reliability of the simulation is also verified by computing the time-of-flights for doubly charged clusters. Again, a good accordance with the experiment is obtained. Considering the agreement of experimental and simulated flight times, the residence time of the parent ions in the first field-free region can be computed. A metastable reaction rate is then obtained by integrating the parent and daughter peaks from the time-of-flight spectrum and taking into

account the simulated residence times in the first field-free region as will be discussed in more detail below.

RESULTS AND DISCUSSION

A. Femtosecond ionization of $(H_2O)_n$ and $(D_2O)_n$ clusters

Figure 1 displays a typical time-of-flight mass spectrum of water clusters ionized by using the 780 nm femtosecond laser pulses. By applying a gated electric field for several μs after the acceleration, the water monomer and a fraction of the dimer ions are deflected to prevent an overload of the microchannel plate detector. The gated region between 10.5 and 58.0 μs is indicated on the Figure 1.

The protonated water cluster ions, $(H_2O)_nH^+$, that are produced in the source region by fast proton transfer dominate the spectrum in the small cluster size region up to n≈15. They appear at flight times that are proportional to the square root of their corresponding mass as indicated on the scale on the top of the Figure 1. An overall smooth exponential decrease of protonated parent cluster intensities *versus* size is observed. With increasing cluster size, daughter ions from unimolecular dissociation in the first field-free region of the reflectron mass spectrometer emerge. These daughter ions can be separated from the parent ions by adjusting the reflectron potentials and are assigned by comparison with trajectory simulations (see below). For the experiment shown in Figure 1 daughter ions appear at lower time-of-flights in respect to the parent signals. This feature is shown more clearly on the insets for n=10 and 16, where the parent and daughter ions are labeled by P and D, respectively. It can be seen that unimolecular dissociation is more abundant for larger clusters sizes. For n=10, the ratio of the daughter to parent ion is ≈ 0.3 and roughly unity for n=16. The daughter peak at n=21 clearly dominates the time-of-flight mass spectrum at ≈ 191 μs (compare also to Figure 3). A closer inspection of the daughter intensities at n=21 and n=22 reveals a local discontinuity in the mass spectrum. This intensity anomaly is attributed to an increased stability towards evaporation of $(H_2O)_{21}H^+$ in respect to $(H_2O)_{22}H^+$. This observation is in agreement with experiments using electron impact ionization in combination with reflectron mass spectrometry [2]. The clathrate cage structure [9] of the 21-mer is more stable against evaporative loss than the cluster containing an additional H_2O molecule.

In addition to singly charged protonated water clusters, doubly charged cluster series of the form $(H_2O)_nH^{++}$ ($n \geq 37$) are also observed at flight times > 180 µs. An example of a doubly charged cluster with n=51 is indicated in the Figure 1. Due to its mass to charge ratio, $(H_2O)_{51}H^{++}$ appears between the two singly charged clusters of the size n=25 and 26.

Similar cluster series are obtained by applying the frequency tripled (260 nm) output of the femtosecond-laser for ionization. Experiments performed at 390 nm by doubling the fundamental frequency of the laser failed to produce acceptable cluster signals. Poth *et al.* [10] have recently reported that it has not been possible to ionize pure water clusters with 100 fs pulses at 400 nm (0.7-1.0 mJ per pulse). The authors did not report, however, whether experiments have been performed at a different wavelength. In this work, a detailed study of the cluster distribution as a function of ionization wavelength has not been attempted. The results reported are obtained by using infrared photons at 780 nm which yield a maximum signal to noise ratio.

In general, a cluster ion mass spectrum produced by a femtosecond laser pulse shows only parent ions and ionic fragments that are produced in the source region and is free of photo-ionized neutral fragments. This is because the 100 fs pulse duration is much shorter than the cluster fragmentation time. An exception is the presence of H^+ in Figure 1 that can be explained by rapid ejection of neutral H atoms and subsequent ionization [11]. However, the reaction producing the H^+ signal is not characterized in the framework of this investigation. Experiments performed at different laser intensities have shown that even by increasing the laser pulse energy by a factor of five, the relative distribution of the cluster signals did not change significantly. In particular we do not observe a shift of the cluster ion mass distribution toward lower masses for increasing laser intensities. This finding is rationalized by considering the previously mentioned vertical ionization process. A point on the ion potential surface is reached from which proton transfer relaxation, cluster rearrangement and subsequent evaporation of water monomer units on the µs time scale occurs. The rapid ionization prevents significant intramolecular energy transfer that would lead to excitation and/or fragmentation of intermediate states. This behavior is very characteristic of the so called ladder climbing mechanism [12] which is expected for femtosecond ionization of polyatomic molecules. In this case, several photons are absorbed subsequently on a very short time scale. The ladder of energy excitation is climbed with a rate that is much higher than the intramolecular energy transfer rate. Due to this rapid process, vertical ionization from the ground state to the potential energy surface of the ion, $[(H_2O)_n^+]^*$, is achieved (Equation 1).

Furthermore, since intramolecular energy transfer in intermediate states is not expected during ionization, cluster heating in femtosecond photoionization is likely to be insignificant. In fact, recent investigations on the photoionization of large molecules using femtosecond excitation pulses have shown that no fragmentation occurs, even with varying the pulse intensity over several orders of magnitude [13]. This findings are in contrast to the nanosecond time regime where it is observed for alkali [14] and ammonia clusters [15] that after photoionization of neutrals, there is a shift of the cluster mass distribution towards lower masses for increasing laser intensities. In this case, the ladder switching mechanism occurs which gives rise to fragmentation and subsequent photon absorption from the excited-state neutral or parent ion within the laser pulse width.

Even though the femtosecond ionization is expected to yield ions exhibiting little excess energy, we have to take into account that the Franck-Condon driven vertical ionization of water clusters probably occurs to a point on the potential energy surface of the ion that is above the proton transfer barrier. The fast proton transfer followed by a rearrangement of the protonated cluster ion produces metastable species that decay in the first field-free region of the mass spectrometer (see below). It is interesting to compare these results with the femtosecond ionization work on ammonia clusters by Castleman and his group [16]. As for the water clusters, the ionization of ammonia clusters result primarily in the formation of the protonated cluster, $(NH_3)_nH^+$, series. However, by applying an ultrafast radiation source for multiple photon ionization an appreciable fraction of the unprotonated cluster ions, $(NH_3)_n^+$, can be formed. The presence of unprotonated ammonia clusters upon femtosecond ionization is rationalized by considering the inherently broad spectral distribution due to the uncertainty relation. Furthermore, multiple photon absorption during the ladder climbing process leads to an effective shortening of the temporal profile and produces an experimental pulse width that is considerably shorter than the instrumentally measured pulse width of the 780 nm laser light. As a consequence, a substantial spectral broadening is expected and gives rise to the population of various vibrational ion states, of which some lie below the proton transfer barrier.

However, in the present investigation of the water clusters, unprotonated species of the form $(H_2O)_n^+$, have not been observed with the exception of the dimer ion, $(H_2O)_2^+$. This result suggests that in contrast to the ammonia cluster work by Castleman and coworkers, vertical ionization of water clusters does not lead to a significant population of the potential energy surface

below the aforementioned barrier. Previously, Shiromaru *et al.* [17] have determined the appearance potentials for $(H_2O)_2^+$, $(H_2O)_3^+$, $(H_2O)_2H^+$, $(H_2O)_3H^+$ by synchrotron radiation. The results suggest that water clusters are directly ionized since the photoionization efficiency curve of H_2O^+ shows no distinct autoionization structure. Furthermore, it has been found that in contrast to the $(H_2O)_2^+$ ion, $(H_2O)_3^+$ is not observed from the water trimer, because the Franck-Condon region covers a smaller part of the potential minimum for the water trimer ion as compared to that for the dimer ion. As for the threshold ionization by synchrotron radiation, the assumption of a Franck-Condon restricted direct vertical ionization by the ladder climbing mechanism is in agreement with our results and rationalizes the lack of unprotonated water clusters.

Additional experiments have been performed on D_2O instead of H_2O molecular beams to shed more light on the proton transfer mechanism. In fact, a substantial change in the zero point energy is introduced by replacing the hydrogen atoms by deuterium due to the different mass. On the other hand, the ionization potentials of H_2O and D_2O are essentially equal (12.7 ± 0.1 and 12.75 ± 0.1 eV, respectively [18]). Figure 2 shows typical mass spectra which are obtained by the femtosecond ionization of a D_2O supersonic molecular beam. The mass of the protonated cluster is subtracted from the mass scales shown in Figure 2. Thus, the signal of the fully deuterated $(D_2O)_nD^+$ cluster appears at the origin whereas an unprotonated $(D_2O)_n^+$ ion would appear at $\Delta m = -2$ amu. Unfortunately, mixed D/H clusters are formed due to a trace amount of light water in the gas inlet system and have to be taken into account. Figure 2 depicts typical mass spectra for n=6, 8, 11 and 17 (dotted line). Additionally, simulations are shown (solid line) that assume a hydrogen to deuterium ratio of 0.02 in the cluster of size n. Intensity normalization is performed with respect to $(D_2O)_nD^+$. The resulting close match of the comparison suggests that the peak at $\Delta m = -2$ amu is mainly due to the exchange of two deuterium atoms by hydrogen in the $(D_2O)_nD^+$ cluster and that unprotonated $(D_2O)_n^+$ ions are not formed in significant quantities. Discrepancies in the mass range above the fully deuterated $(D_2O)_nD^+$ clusters are due to metastable fragmentation products (see below). Thus, we conclude that the change in zero point energy does not lead to a more favorable Franck-Condon overlap of the neutral and ion state. As for light water, ionization takes place primarily to a point above the proton transfer barrier according to Equation 1.

More light is shed on the ionization mechanism by a study of the log(ionization signal) *versus* log(laser power). The investigation for ammonia clusters [16] yields a slope of 4 for

$(NH_3)_nH^+$, $1 \leq n \leq 5$, indicating that ionization is achieved through a four-photon resonant intermediate state that corresponds to the C'(v=1) state of the ammonia monomer. A power dependence study in this work on the $(H_2O)_nH^+$ cluster ions also results in a slope of ≈4. By considering the spectral broadening of multiphoton transitions as discussed above, the intermediate state for the photoionization of water clusters at 780 nm is most probably corresponding to the Â state of the water monomer at 185.9 nm.

After the water clusters are ionized, the proton transfer has occurred and a neutral OH is lost in the acceleration region of the mass spectrometer, unimolecular dissociation of the metastable protonated clusters takes place by loss of one or more water monomers. Such a relaxation reaction has been observed upon electron impact ionization of the $(H_2O)_n$ clusters [2], and is similar to the metastable behavior of the protonated $(NH_3)_nH^+$ series upon nanosecond ionization techniques [19]. The characterization of the metastable dissociation of $(H_2O)_nH^+$ upon femtosecond ionization in the following section draws strongly from these works.

B. Unimolecular dissociation of metastable $(H_2O)_nH^+$ and $(D_2O)_nD^+$ clusters

The multiphoton ionization method used in our experiment is a "hard" ionization so that possible ionization potential differences should not make much difference in ionization cross sections of these clusters [20]. This situation is completely different from electron impact and nanosecond ionization where ionization efficiencies are strongly dependent on cluster size. Thus, it is assumed that the spectra shown in Figure 1 and in more detail in Figure 3 represent cluster ion series which have been ionized with equal efficiencies. The overall exponential decay of the parent cluster intensities *versus* size reflects the abundance of the neutral clusters produced by the supersonic expansion. However, local discontinuities are measured due to metastable reactions of the clusters in the first field-free region. The daughter ions from the dissociation are also observable and appear as satellite peaks for parent clusters with n>6 (Figure 1). As mentioned above, this sequential evaporative loss of monomers and dimers following femtosecond irradiation is mainly due to the configurational energy imparted into the protonated cluster ions. An extended view of the time-of-flight spectrum is depicted in Figure 3 (solid trace). In addition, ion trajectory simulations are shown (dotted trace). The computed time-of-flights are convoluted with a Gauss

function exhibiting a FWHM of the mass spectrometer resolution. The intensities are computed by assuming an exponential distribution of the protonated parent cluster sizes in the ionization region and by taking into account the metastable dissociation rates during the flight time in the first field-free region (see below). Small discrepancies might origin from the kinetic energy release of the metastable dissociation process that is neglected in the modeling of the ion trajectories. However, the simulations confirm the suggested origin of the satellite peaks observed in the time-of-flight spectra. They occur due to evaporation of water molecules, i.e.,

$$(H_2O)_nH^+ \rightarrow (H_2O)_{n-1}H^+ + H_2O. \qquad (3)$$

The spectrum shown in Figure 3 also reveals the loss of two water molecules for larger clusters. It has been shown that the binding energy of an additional H_2O to an ion of the form $(H_2O)_nH^+$ decreases from 1.47 eV for n=1 to 0.87 and 0.74 eV for n=2 and 3 respectively [21], which may favor additional monomer losses with increasing cluster size.

It is important to notice that the observed metastable fragmentation takes place during the flight through the first field-free region of the reflectron time-of-flight mass spectrometer. Interactions with the background gas can lead to collision-induced dissociation and blur the real metastable decay process. However, at a pressure of $\approx 2.5 \times 10^{-8}$ Torr, as indicated on an ion gauge mounted at the entrance to one of the turbo pumps of the reflectron, collision induced dissociation is expected to be minimal and its contribution to the metastable dissociation negligible.

The range of times over which unimolecular dissociation can be observed, and thus the range of rate constants that may be detected, depends on the physical dimensions of the apparatus and the kinetic energy of the ion beam. The ion trajectory simulations show that the available experimental setup allows observation of metastable lifetimes in a time window of 30-60 µs, depending on the mass of the cluster ion. By assuming a single exponential decay process, the observed relative integrated fragment to parent intensities I_f/I_p can be converted into a metastable rate constant k by the relation:

$$I_f/I_p = [\exp(k\, t_{ff}) - 1] \exp(k\, t_{ref}) \qquad (4)$$

where the first factor describes the decay during the travel time t_{ff} in the first field-free region of the mass spectrometer and the second exponential corrects for further fragmentation of the parent ions while passing the reflector (t_{ref}). Values for t_{ff} and t_{ref} are available from the ion trajectory calculations. Figure 4 shows the resulting rate constants k for $8 \leq n \leq 18$. The indicated error bars are standard deviations from 4 consecutive measurements. The mass spectrometer resolution is insufficient to compute accurate rate constants for the larger clusters. For the small size region the accuracy is limited due to small parent signals. In the observed cluster size range an overall smooth increase towards n = 12 is obtained that levels off for larger clusters at a value of ≈12000 s^{-1}. The rate constants for $13 \leq n \leq 18$ imply little variations in binding energies and possibly also in structures for this size range. It is interesting to compare the results with the decay fractions of protonated water clusters reported by Shi *et al.* [22]. The authors applied nanosecond ionization to a mixed cluster beam containing H_2O/CH_3I and measured the decay fractions $I_f/(I_f+I_p)$ of protonated water clusters. Besides of the pronounced maximum at the 22-mer due to the enhanced dissociation to the more stable 21-mer, an overall steep increase to n = 12 is found that levels off somewhat for the larger cluster sizes, which is in agreement with our observations.

C. Unimolecular dissociation of doubly charged $(H_2O)_nH^{++}$ and $(D_2O)_nD^{++}$ clusters

Dissimilar to electron impact and near-threshold ionization, doubly charged species appear in the mass spectra at flight times above ≈ 180 μs (Figure 1). The trajectory simulations shown in Figure 3 indicate that the doubly charged mass peaks emanate most probably from the unimolecular dissociation reactions

$$(H_2O)_nH^{++} \rightarrow (H_2O)_{n-1}H^{++} + H_2O \qquad (5)$$

and

$$(H_2O)_nH^{++} \rightarrow (H_2O)_{n-2}H^{++} + 2(H_2O) \qquad (6)$$

Unfortunately, the simulations do not reveal whether Reaction 6 proceeds by subsequent or simultaneous loss of two monomers. Note, that in contrast to the singly charged clusters, only daughter ions are detected. The rapid unimolecular dissociation process during the flight time in

the first field-free region consumes the parent clusters completely. Thus, mass calibration relies solely on the doubly charged daughter ions and is insufficient to acertain a difference of one mass unit in this mass range. As a consequnce, parent ions of the form $(H_2O)_nH_2^{++}$ that evaporate water molecules might be considered as an interesting alternative.

To our knowledge neither doubly charged water nor ammonia cluster series have been observed previously. However, direct evidence has been reported of Coulomb explosions of multiply charged ammonia clusters upon the interaction with an intense femtosecond laser beam that yield singly charged cluster series [23]. Generation of multiply charged polyatomic molecules in intense infrared laser beams in the femtosecond time regime has been investigated very recently [24]. The authors conclude that the molecules reach the 1^+ ion level by multiphoton processes during the rise time of the pulse. For laser intensities approaching 10^{14} W cm^{-2}, they absorb more photons sequentially and reach multiply charged levels either by tunneling ionization or by barrier suppression. Below a critical size ($n<37$), we do not observe doubly charged species in the mass spectrum due to the strong repulsive Coulomb forces resulting in fission. As for the larger clusters, the excess energy imparted in generating multiply charged clusters also stimulates extensive evaporation. Thus, we rationalize the observed critical size as the first cluster in the decay sequence for which the lifetime for fission is comparable to the evaporation lifetime.

SUMMARY

Femtosecond multiphoton ionization has been applied to H_2O and D_2O clusters generated in a supersonic molecular beam. The use of ultrashort laser pulses is advantageous since the ionization process occurs on a time scale that is substantially shorter than the molecular dissociation time. Furthermore, the high intensity of the laser pulses is sufficient to ionize most of the neutral species abundant in the molecular beam. As a consequence, large water clusters up to $n \approx 60$ are observed. Due to rapid proton transfer of the vertically ionized water clusters prior to the acceleration in the reflectron time-of-flight mass spectrometer, only protonated water clusters are found in the mass spectra. The absence of $(H_2O)_n^+$ clusters suggests that vertical ionization does not populate ion states that are below the proton transfer barrier. This result is in contrast to the femtosecond ionization of ammonia clusters where unprotonated cluster ions are also observed [16]. Additional experiments performed with deuterated water did not result in

unprotonated $(D_2O)_n^+$ species even though a substantial change in the zero point energy is expected.

The vertical ionization and proton transfer process leaves the protonated water clusters with a broad range of energies which permit evaporation. The unimolecular decay in the first field-free region of the reflectron time-of-flight mass spectrometer is analyzed by comparing the mass spectra with ion trajectory calculations and yields rate constants as a function of cluster size.

Furthermore, doubly charged water clusters are also present in the mass spectra. A comparison with the simulations reveals that the ion signals are due to daughter ions formed by metastable dissociation of doubly charged parent clusters loosing one or two neutral monomers. The clusters appear above a critical size of $n>37$. The observation of a threshold to form doubly charged clusters suggests that small species dissociate rapidly due to the strong Coulomb forces whereas larger doubly charged clusters are stabilized by extensive evaporation.

ACKNOWLEDGEMENT

Support of this work by the Swiss Federal Office of Energy (BFE) is gratefully acknowledged. We are grateful to the referee for the critical reading of the manuscript and the helpful suggestions.

FIGURE CAPTIONS

Figure 1 Time-of-flight spectra obtained upon femtosecond photoionization at 780 nm of a supersonic molecular beam containing water clusters. Series of protonated water cluster ions, $(H_2O)_nH^+$, are observed. Parent ions are produced by fast proton transfer in the source region of the mass spectrometer (*P*). Daughter ions (D) originate from metastable decay in the first field-free region. Corresponding cluster sizes n are indicated at the top of the figure. In addition, doubly charged cluster series, $(H_2O)_nH^{++}$, are observed for n (n≥37) An electric field is applied to deflect the monomer and a fraction of the dimer ion to prevent an overload of the detector.

Figure 2 Mass spectra of deuterated water clusters with n=6,8,11 and 17 upon femtosecond photoionization at 780 nm (dotted). Simulation of the mass spectra by assuming a H/D ratio of 0.02 (solid). The ordinate and the abscissa are normalized to the fully deuterated $(D_2O)_nD^+$ intensity and mass, respectively. The good agreement of the simulation suggests that the peaks occurring at $\Delta m = -2$ amu are mainly due to the exchange of two deuterium atoms by hydrogen in the $(D_2O)_nD^+$ cluster and that unprotonated $(D_2O)_n^+$ ions are not formed in significant quantities.

Figure 3 Expanded region of the time-of-flight mass spectrum (solid). Parent clusters, $(H_2O)_nH^+$, are produced in the source region. The remaining ion signals occur due to the metastable decay in the first field-free region. The separation of the parent/daughter time-of-flights is achieved by adjusting the reflector potentials. Ion trajectory simulations are performed for singly and doubly charged protonated clusters and are shown (dotted) for comparison. Small discrepancies might be due to the kinetic energy release of the metastable dissociation which is omitted in the simulation. See text for details.

Figure 4 Fragmentation rate constants for protonated water cluster ions. The rates are computed from the integrated parent and daughter intensities and by taking into account the residence time in the first field-free region from the modeling of the ion trajectories. Error bars are standard deviations from 4 measurements. See text for details.

REFERENCES

[1] V. Hermann, B. D. Kay, and A. W. Castleman Jr., Chem. Phys. **72**, 185 (1982).

[2] O. Echt, D. Kreisle, M. Knapp, and E. Recknagel, Chem. Phys. Lett. **108**, 401 (1984); D. Kreisle, O. Echt, M. Knapp, and E. Recknagel, Surf. Sci. **156**, 321 (1985).

[3] M. Tsuchiya, E. Aoko, and H. Kuwabara, Int. J. Mass Spectrom. Ion Proc. **90**, 55 (1989).

[4] H. Haberland, in *Electronic and Atomic Collisions,* edited by J. Eichler, I. V. Hertel, N. Stolterfoht (Elsevier Science Publishers, City, 1984), pp. 597-605.

[5] S. Tomoda and K. Kimura, Chem. Phys. **82**, 215 (1983).

[6] H. Shinohara and Nobuyuki Nishi, J. Chem. Phys. **84**, 5561 (1986).

[7] M. J. DeWitt and R. J. Levis, J. Chem. Phys. **102**, 8670 (1995).

[8] SIMION 3D, Version 6.0, Idaho National Engineering Laboratory, Idaho Falls, USA.

[9] S. Wei, Z. Shi, and A. W. Castleman, Jr., J. Chem. Phys. **94**, 3268 (1991).

[10] L. Poth, Z. Shi, Q. Zhong, and A. W. Castleman, Jr., Int. J. Mass Spectrom. Ion Proc. **154**, 35 (1996).

[11] R. Weinkauf, P. Aicher, G. Wesley, J. Grotemeyer, and E. W. Schlag, J. Phys. Chem. **98**, 8381 (1994).

[12] A. Gedanken, M. B. Robin, and N. A. Kuebler, J. Phys. Chem. **86**, 496 (1982).

[13] S. Wei, J. Purnell, S. A. Buzza, R. J. Stanley, and A.W. Castleman Jr., J. Chem. Phys. **97**, 9480 (1992).

[14] C. Bréchignac, Ph. Cahuzac, and J.-Ph. Roux, J. Chem. Phys. **88**, 3022 (1988).

[15] S. Wei, W. B. Tzeng, and A. W. Castleman, Jr., J. Chem. Phys. **93**, 2506 (1990).

[16] S. A. Buzza, S. Wie, J. Purnell, and A. W. Castleman, Jr., J. Chem. Phys. **102**, 4832 (1995).

[17] H. Shiromaru, H. Shinohara, N. Washida, H.-S. Yoo, and K. Kimura, Chem. Phys. Lett. **141**, 7 (1987)

[18] T. D. Märk, and F. Egger, Int. J. Mass Spectrom. Ion Phys. **20**, 89 (1976).

[19] S. Wei, W. B. Tzeng, and A. W. Castleman, Jr., J. Chem. Phys. **92**, 332 (1992).

[20] L. Poth, Z. Shi, Q. Zhong, and A. W. Castleman, Jr., J. Phys. Chem. **101**, 1099 (1997).

[21] K. Honma, L. S. Sunderlin, and P. B. Armentrout, J. Chem. Phys. **99**, 1623 (1993).

[22] Z. Shi, J. V. Ford, S. Wei, and A. W. Castleman, Jr., J. Chem. Phys. **99**, 8009 (1993).

[23] D. A. Card, D. E. Folmer, S. Sato, S. A. Buzza, and A. W. Castleman, Jr., Phys. Chem. A, **101**, 3417 (1987); E. M. Snyder, S. We, J. Purnell, S. A. Buzza, A. W. Castleman, Jr., Chem. Phys. Lett., **248**, 1 (1996).

[24] K. W. D. Ledingham, R. P. Singhal, D. J. Smith, T. McCanny, P. Graham, H. S. Kilic, W. X. Peng, S. L. Wang, A. J. Langley, P. F. Taday, and C. Kosmidis, J. Phys. Chem. A, **102**, 3002 (1998).

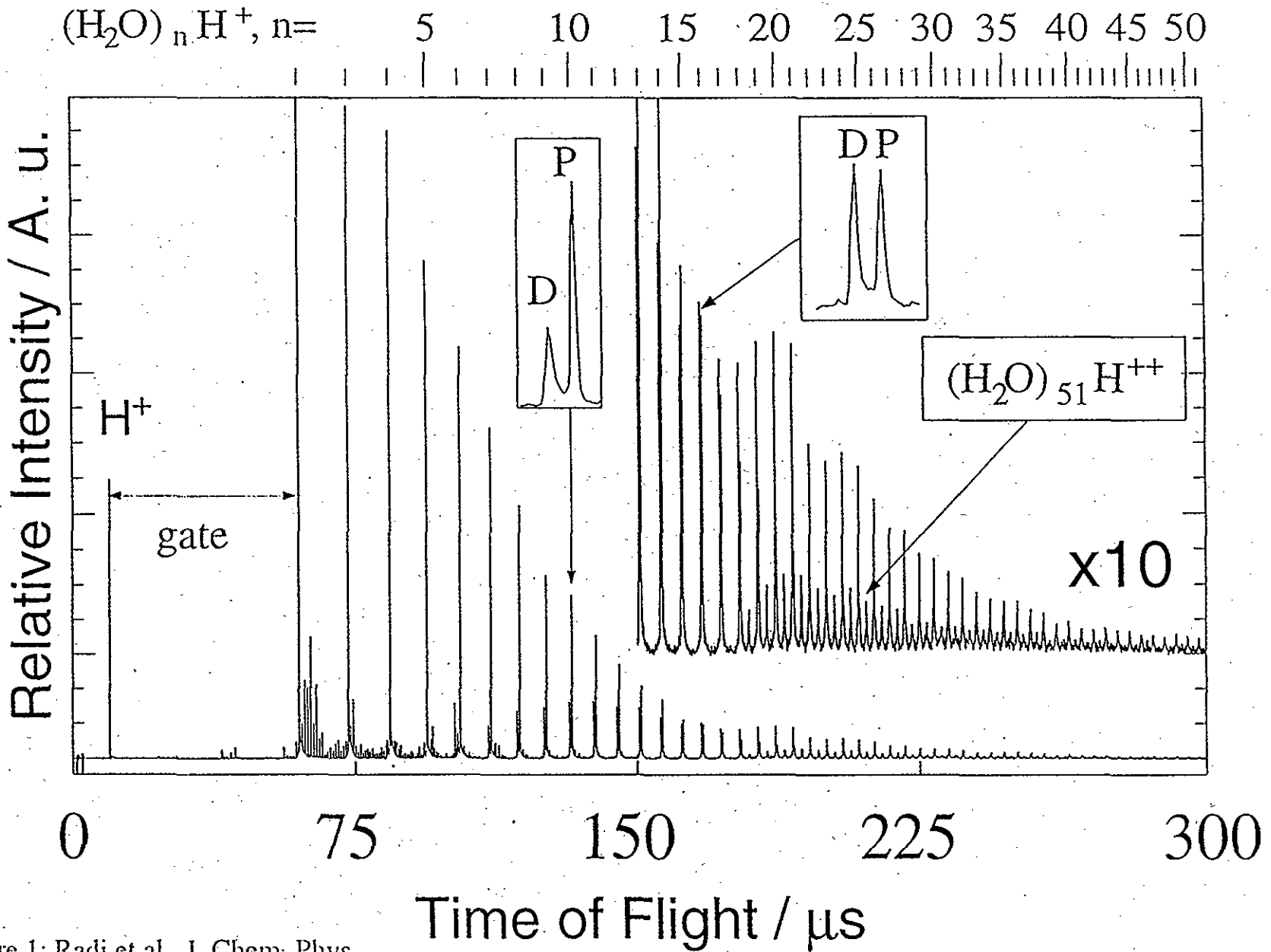

Figure 1: Radi et al., J. Chem. Phys.

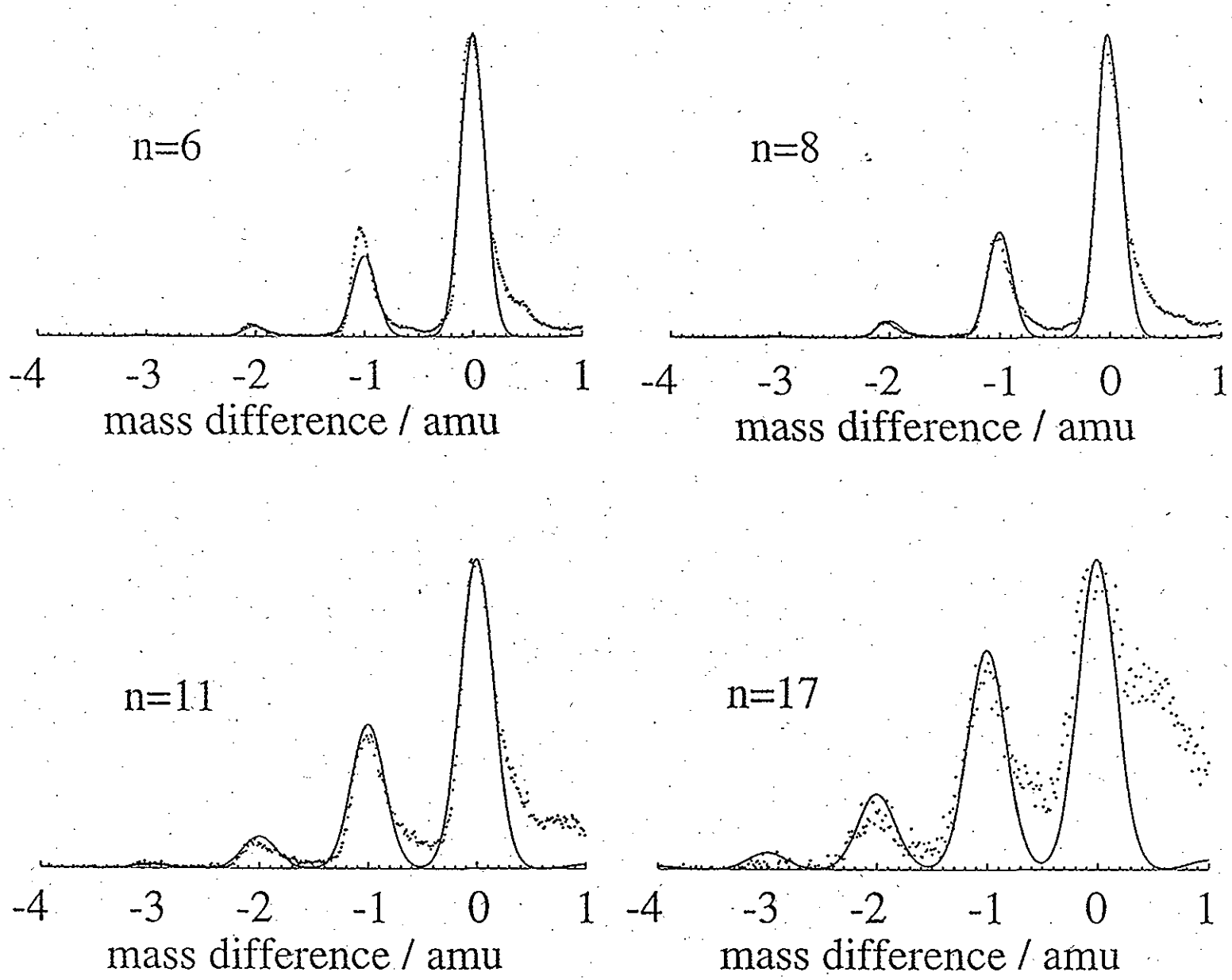

Figure 2: Radi et al., J. Chem. Phys.

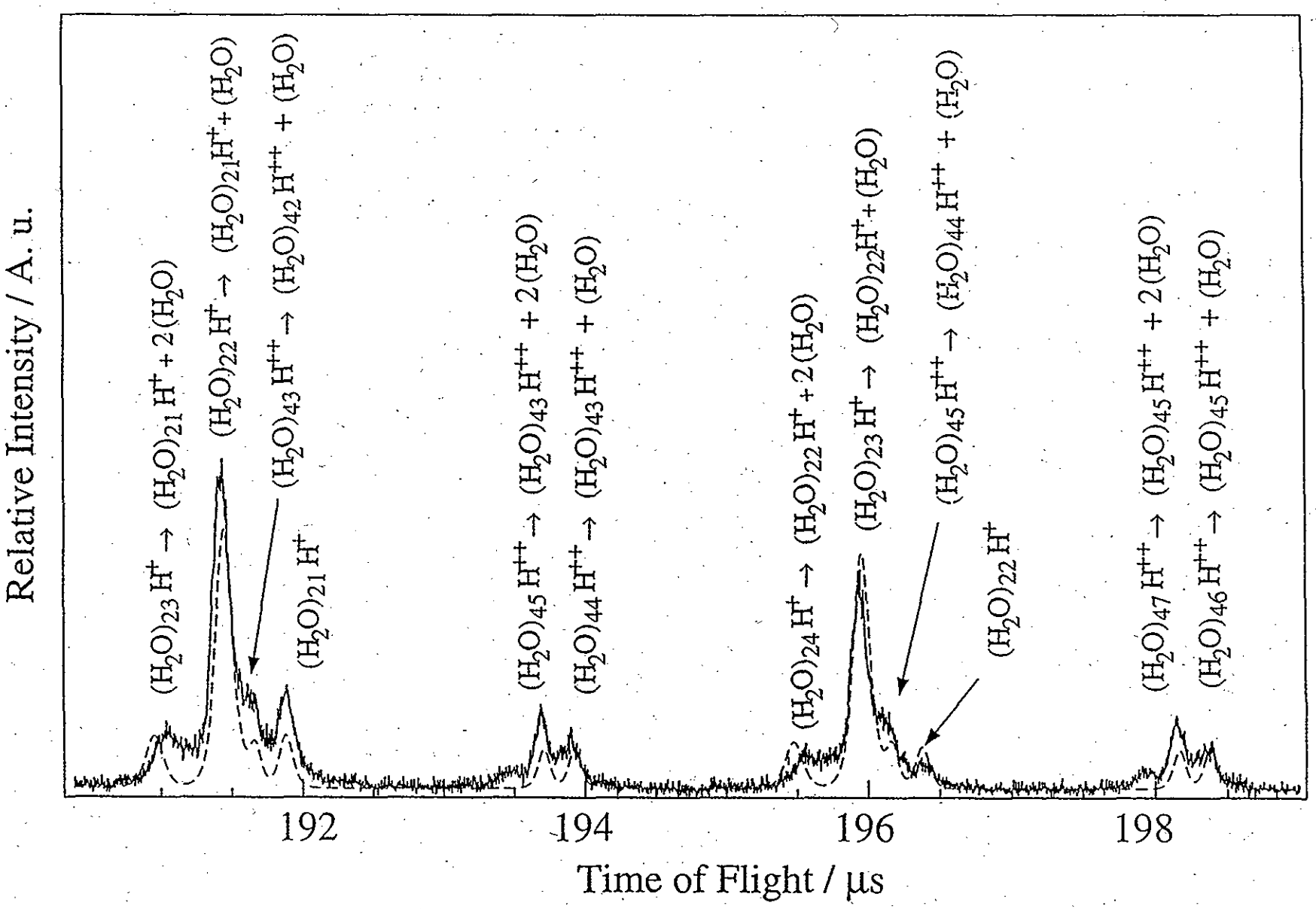

Figure 3: Radi et al., J. Chem. Ph

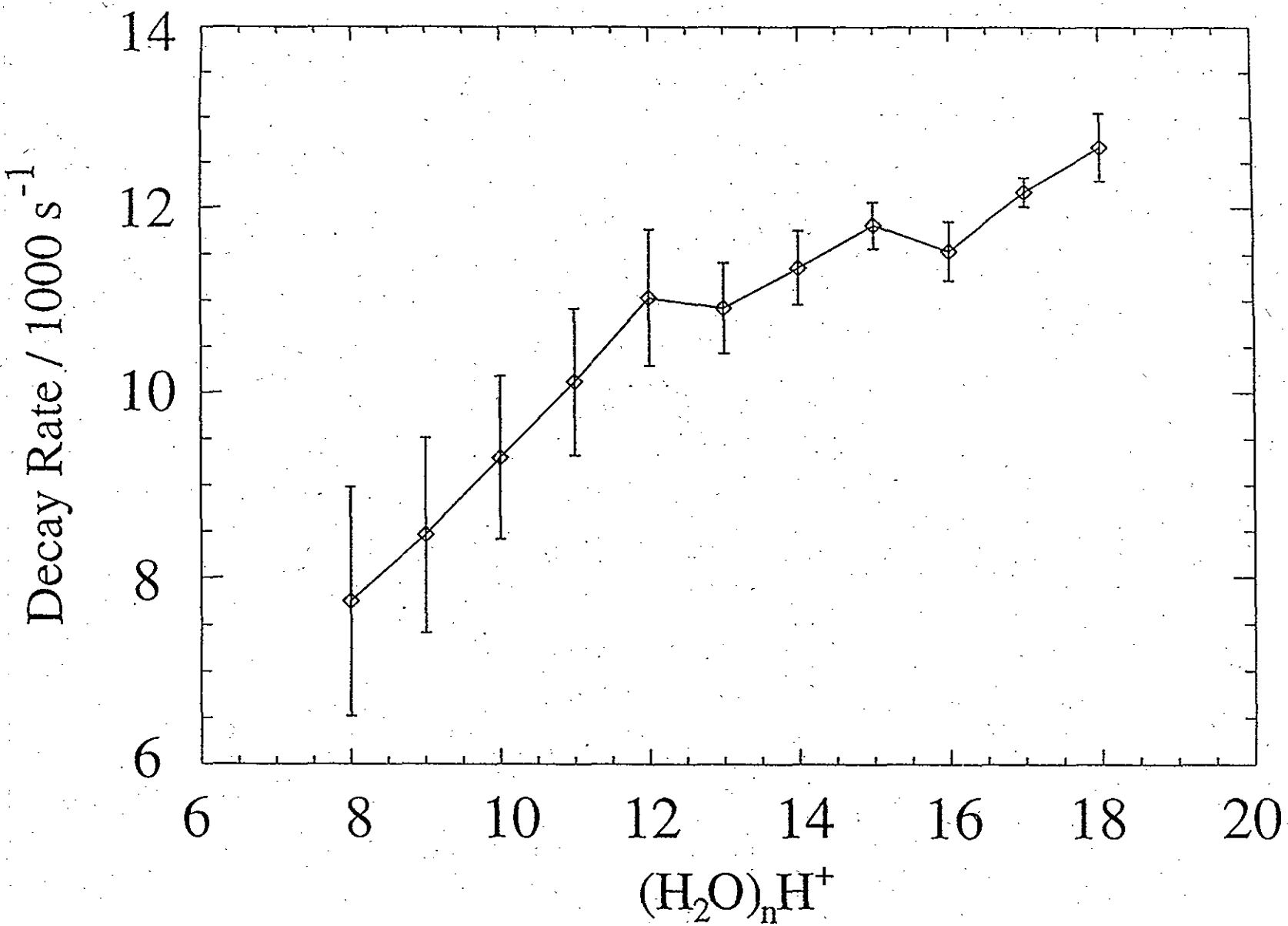

Fig. 4: Radi et al, J. Chem. Phys.